Exp. Theo. NANOTECHNOLOGY 9 (2025) 273-286 https://doi.org/10.56053/9.S.273

NaI concentration effect on physical characteristic of poly vinyl alcohol: Sodium iodide nano films for gas sensors

Mahdi Hasan Suhail[1,], Zina A. Al Shadidi[2], Qudama Kh. Hammad[3], Saja Neama Kareem[4]*

[1,3]Al Ma'moun University College, Department of Medical physics, Baghdad, Iraq
[2]Al Ma'moun University College, Department of of Radiology, Baghdad, Iraq
[4]Baghdad University, Science College, Department of Physics, Baghdad, Iraq
[*]) Email: mahdi.h.suhail@almamonuc.edu.iq

Received 21/1/2025, *Received in revised form* 3/2/2025, *Accepted* 19/2/2025, *Published* 15/3/2025

The sodium Iodide nanoparticles are added to polyvinyl alcohol with different concentrations at (10, 20,30 and 40) wt.% . The preparation and performance of the blends are prepared by the casting method. The structural morphology is characterized using X-ray diffraction (XRD), furriertransform infrared spectroscope (FTIR) and atomic force microscopy (AFM). The result showed a uniform blend of PVA with NaI matrix. The prepared nanocomposites are characterized using UV–VIS spectrophotometer and the optical properties showed that as NaI contents increased to 40% weight, the films' direct allowed optical energy are investigated in the wavelength range 300-1100 nm. The collected results gap decreased from 4.27 to 4.22. The electrical conductivity and activation energy are calculated. Effect of temperature on electrical conductivity are also investigated. Furthermore, in order to understand the behavior of electrical conductivity in these composites, the alternating electrical conductivity and dielectric permittivity have been investigated for different concentration of NaI at room temperature over the frequency ranging from to 1Hz -10 kHz. The electrical conductivity of the composite increased with increasing temperature and it obeys power law in which s is in the range of 0.99- 0.084 s the sensing properties are evaluated to ascertain the effects of NaI on the sensitivity, selectivity, and response/recovery time of PVA/NaI nanocomposite films. The maximum sensitivity (S) of 127.3 % towards NO_2 gas detection at a 50 ppm concentration at temperature 473K with response/recovery times of ~ 25/25 s is observed for nanocomposites with 20 wt% NaI loading in a PVA matrix.

Keywords: Electrolyte composite; Optical; Dielectric constant; Energy gap.

1. INTRODUCTION

The basic approach to convert polymers from insulator to conductor form is by using conducting fillers, such as metallic powders and fibres, carbon nanotube, graphene, and conducting polymer (S. Geetha, K.K. Satheesh, K. Chepuri, R.K. Rao, M. Vijayan, D.C.Trivedi, 2009) (Shirale, D. J., Gade, V. K., Gaikwad, P. D., Kharat, H. J., Kakde, K. P., Savale, P. A., Hussaini, S. S., Dhumane, N. R., Shirsat, M. D., 2006)Attempts have been made to produce composites or blends of conducting polymer films with some insulating polymer in order to overcome the drawbacks such as poor process ability and the lack of essential mechanical properties exhibited by these polymers. Blending insulating polymers is an attractive route to improve their mechanical properties without losing their conductivity. Polyvinyl alcohol (PVA) is a water-soluble synthetic polymer, its molecular formula is $(C_2H_4O)_x$, and density is between 1.19 and 1.31 g/cm^3. PVA has excellent film forming and adhesive properties. With higher humidity more water is absorbed, which acts as a plasticizer, and will then reduce its tensile strength.
Some uses of PVA include: thickener, modifier, textile sizing agent paper coatings and release liner. When doped with iodine, PVA can be used to polarize light, and is not prepared by polymerization of the corresponding monomer. PVA/NaI combination will improve the conductivity properties of the polymer due to the conductivity of polyvinyl alcohol. Various applications of conducting polymers in diverse fields have been proposed as transducers for biosensors (C. Jo, D. Pugal, I.K. Oh, K.J. Kim, K. Asaka, 2003),electrodes of rechargeable batteries (M. Yu, H. Shen, Z.D. Dai, 2007), artificial nerves and muscles (K. Balakrishnan, M. Kumar, S. Angaiah, 2014), gas sensors (K. Hu, D.D. Kulkarni, I. Choi, V.V. Tsukruk, 2014), solid electrolytic capacitor, diodes, and transistors (Ansar, 2006), anti-static electromagnetic shielding (P. Banerjee, B.M. Mandal, 1995), and biomedical applications (S. Virji, J. Huang, R.B. Kaner, B.H. Weiller, 2001). The combination of conventional polymers with conductive polymers or fillers is an important alternative to obtain new polymeric materials with designed properties (A.K. Solarajan, V. Murugadoss, S. Angaiah, 2017) (A. M. Meftah, E.Gharibshahi, N. Soltani,W.M. M. Yunus and E. Saion, 2014) (M. khan, A. N. khan, and A.Saboor, I. H. GulInvestigating, 2017).

The relationship between incident intensity and penetrating light intensity is given by (Elliot, 1987):

$$I = I_o e^{-\alpha t} \quad (1)$$

where t is the thickness of matter and α is the absorption coefficient

$$\alpha\, t = 2.303 \log I/I_o \quad (2)$$

The amount of $\log I/I_o$ represents the absorbance (A).
The absorption coefficient can be calculated by:

$$\alpha = 2.303\,(A/t) \quad (3)$$

The extinction coefficient (k) can be calculated by using Equation:

$$k = \alpha\lambda/4\pi \quad (4)$$

where λ is the wavelength of the incident ray.
The refractive index can be expressed by the equation (Mustafa Al-hamdany, Mohamed Ghazi and Mahdi Hasan Suhail , 2016):

$$n = \sqrt{\frac{4R - k^2}{(R-1)^2}} - \frac{(R+1)}{(R-1)} \quad (5)$$

The amount of optical energy gap from this region can be evaluated by the relation (Abeer Mohammed, Mahdi Hasan Suhail and Mohammed Ghazi, 2017):

$$\alpha\, h\upsilon = A(h\upsilon - E_g)^m \quad (6)$$

Where $h\upsilon$ is the photon energy, A is the proportional constant, $E_g$is the allowed or forbidden energy gap of direct transition and m is a constant.

The relation between the complex dielectric constant (*ε)* and the complex refractive index *N* \ (*N* = *n-ik*), is expressed by:

$\varepsilon = N^2$ (7)

It can be concluded that:

$(n\text{-}ik)^2 = \varepsilon_r - i\varepsilon_i$ (8)

The real $\varepsilon_r$and imaginary $\varepsilon_i$complex dielectric constant can be expressed by Equations 11 and 12, respectively:

$\varepsilon_r = n^2 - k^2$ (9)

$\varepsilon_i = 2nk$ (10)

The conductivity values are calculated from the current via the following equation (Mohammed, 2016) (H. Yano, K. Kudo, K. Marumo, H. Okuzaki, 2019):

$$\sigma = \frac{I}{V}\frac{S}{L\,l} \quad (11)$$

where V represents the applied voltage between the electrodes, I is current, S is the width amidst the electrodes, L is the thickness of the sample and l is the length of the electrodes.

The electrical conductivity and temperature can be described by using the Arrhenius equation (M.Z. Rajab, K.M. Ziadan, 2020):

$$\sigma = \sigma_0\, exp - \frac{Ea}{KT} \quad (12)$$

where E_a is the activation energy, K; and the Boltzmann constant is 8.617×10^{-5} eV K^{-1}.

Dielectric constant is determined from the relation (Walsh., 1998):

$$\varepsilon_r = \frac{d\,.C}{\grave{A}\,.\varepsilon o} \quad (13)$$

Whered the distance between electrodes, (C is the capacitance of the sample, A is the effective area (À=width of electrode x thickness of sample), and ε_o is permittivity of the space ($8.854x10^{-12}$ $F.m^{-1}$).

In this work, an attempt has been made to improve conductivity by PVA addition and PVA/NaI preparation with good conductivity, which is suitable for electrolyte materials application.

2. EXPERIMENTAL DETAILS

2.1. Materials and samples preparation

The polyvinyl alcohol (PVA) and sodium iodide (NaI) used in this investigation are provided by Merck Company. A Series of sodium-ion conducting SPE films have been prepared using the solution cast technique. The pure PVA solution is first prepared by dissolving 2 gm of PVA powder in 40 ml double-distilled water using a magnetic stirrer for two hours at a temperature of 80 °C in the water bath to prevent thermal decomposition of PVA. Then, the proper amounts of NaI salt are added to the completely dissolved PVA matrix to prepare sodium-ion conducting SPE films with different salt contents of 10, 20, 30, and 40 wt.%. The mixtures are continuously stirred for an additional hour by a magnetic stirrer. The homogenous viscous solution is then cast onto a 2.5 cm x 7.5 cm glass substrate and stored in a dust-free chamber at room temperature to slowly evaporate the solvent, producing cast films with varying NaI contents. The average thickness of SPE samples ranges between 0.2 and 0.3 μm.

2.2. Characterization techniques

X-ray diffraction is performed using a Bruker D8 Advance diffractometer with CuKα line (λ=1.5418 Å) under operating conditions; voltage 40 kV and current 40 mA. The scattered intensity is collected for 2θ from 10° to 70° with an increment of 0.02° at ambient temperature (30 °C). Computerized Fourier transform infrared spectroscopy (FTIR), from Bruker Alpha Corporation is also used to analyze the bond structure of the present SPE systems in the wavenumber region from 400 to 4000 cm^{-1}.

Atomic force microscope (AFM) scanning probe microscope (SPM) model AA3000, is used to examine the surface morphology for as-prepared SPE films. Micrographs provide data on average roughness, root-mean-square (RMS) roughness, grain size, and particle size distribution throughout the sample surface.

A double beam UV-Visible spectrophotometer (Cecil 2700, provided by the optima 300 plus company) is used at room temperature to record the absorbance and transmittance of SPEs as a function of wavelength over the range 190-1100 nm.

Keithley electrometer model 2400 Source-Meter is used to measure the resistivity as a function of temperatures from 30 to 90 ºC. The DC conductivity of the prepared SPE thin films is investigated using two-point measurements at two locations on the sample with the aid of LabVIEW software.The electrical measurements on the PVA/NaI SPEs are performed in the frequency range of 1 Hz to 100 kHz. The equivalent parallel combination of capacitance, C_p, and resistance, R_p, data at a given frequency are obtained by the LCR meter model Fluke PM6036.

3. RESULTS AND DISCUSSION

3.1 Structural Properties

The X-ray diffraction patterns of pure PVA and PVA complexed with NaI salt, which shows the PVA-NaI film with major amorphous nature. The disappearance of peaks for sodium iodide salt in the complexes indicates that the salt has completely dissolved in the polymer matrix. Higher NaI salt concentrations in the polymer did not show any sharp peak, indicating that amorphous phase predominated (Madhu Mohan, V., Raja, V., Sharma, A. K., and Narasimha Rao, V. V. R.,, 2005). Various study groups also came to similar conclusions (Mohamad, 2003) (Dilip K. Pradhan, 2009) (panelAnil Kumar Bajpai, 2016).

The FTIR spectra for pure PVA, NaI complexed PVA at different compositions salt are shown in Figure 1. All spectra exhibit the characteristic absorption bands of pure PVA composite. It can be noticed that these treatments cause some observable changes in the spectral features of the samples a part from new absorption bands and slight changes in the intensities of some absorption bands. The newbands may be correlated likewise to defects induced by the charge transfer reaction between the polymer chain and the dopant. The following changes in the spectral features have been observed after comparing the spectrum of complexed PVA with that of pure PVA. All these changes in the FTIR spectra are clear indications for the complexation of PVA with NaI (Mohamad, 2003) (Dilip K. Pradhan, 2009).

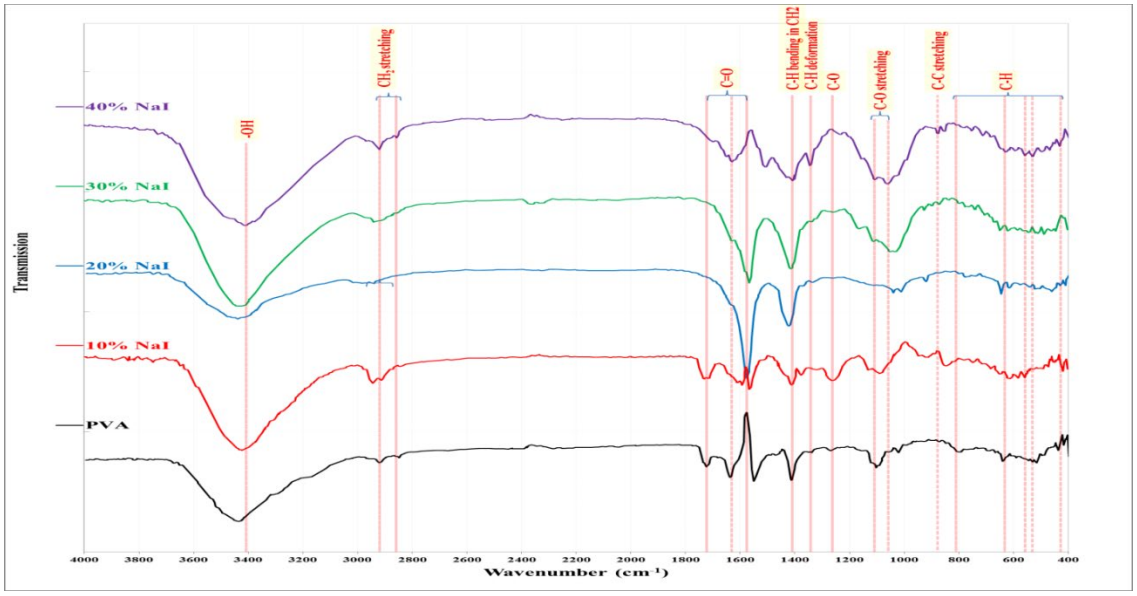

Figure 1 FTIR patterns for pure PVA and that mixed with NaI at different percentages.

AFM provides critical information in the development, optimization, and monitoring of thin film growth processes, and in rationalizing design pathways to achieve desired functional propertiesThe resolution of AFM depends on the structure and material of the AFM nanotip. Figure 2 refers to the 3D representations of the 2 ×2 μm zone and size distribution of PVA-NaI. The average diameter between 10.61and 25.57 nm.

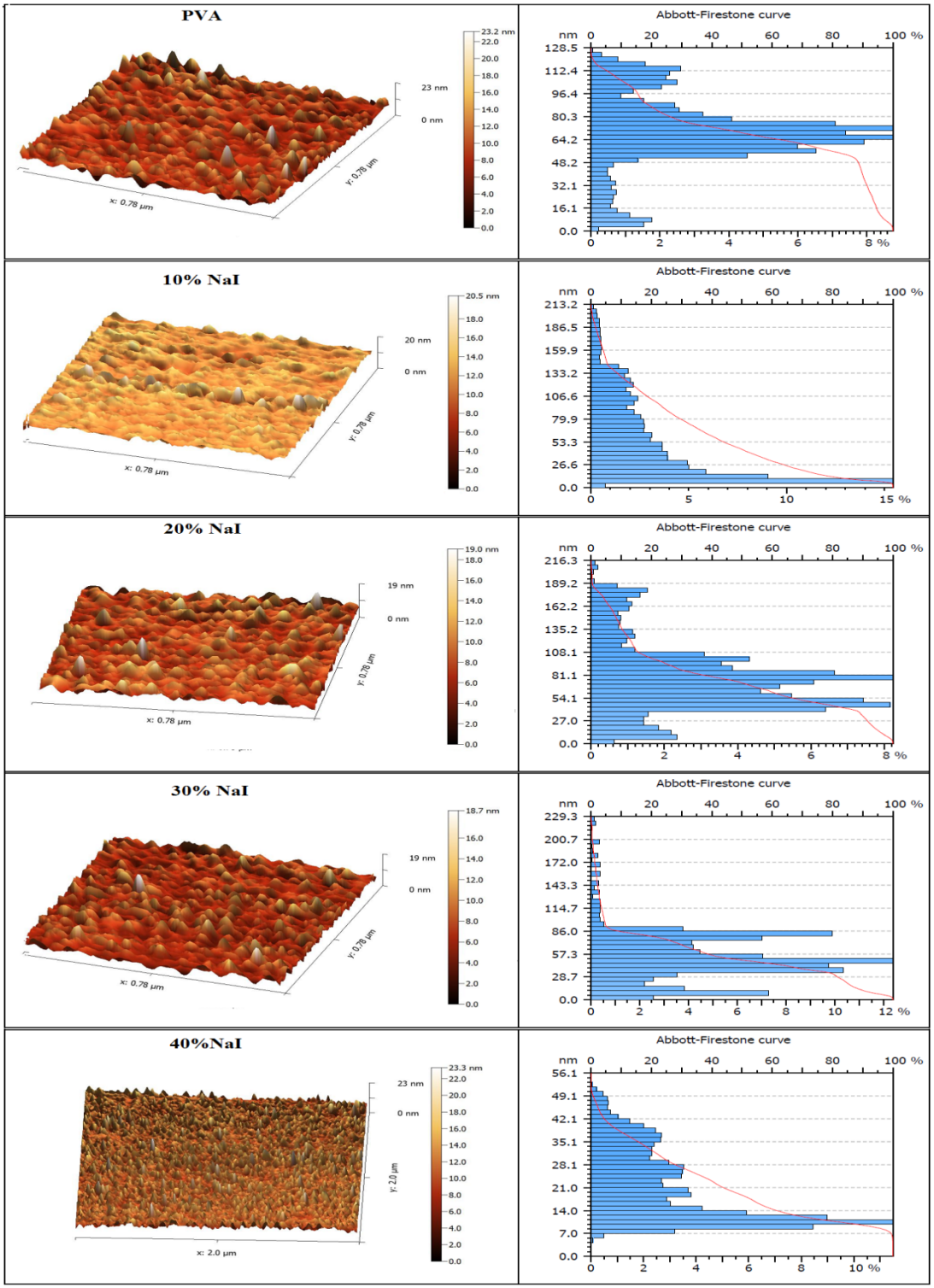

Figure 2 AFM images for pure PVA and mixed with NaI at different percentages.

The AFM parameters for pure PVA and with NaI at different percentages are shown in table 1. The detailed roughness parameters of the above mention films are summarized in Table 1. It is clearly observed from Table 1 and comparative study of R_{ave} and R_{rms}, that as doping of the monomer or polymer takes place inside the PVA film, the roughness of the surfaces decreases i.e. domains of small sizes are formed (panelAnil Kumar Bajpai, 2016)

Table 1 AFM parameters for pure PVA and with NaI at different percentages.

Sample name	Root Mean Square (nm)	Average roughness (nm)	Average diameter (nm)	Particle size (nm)
Pure PVA	2.27	1.7	12.29	72.5
10% NaI	1.50	1.09	25.57	67.84
20% NaI	1.93	1.46	10.64	82.89
30% NaI	1.87	1.42	10.61	58.03
40% NaI	1.64	1.23	17.85	23.33

3.2 Optical properties

The optical properties of SPE are influenced by several factors, such as preparation conditions, surface morphology, type of salt, and concentration (El-Khodary, Evolution of the optical, magnetic and morphological properties of PVA films filled with CuSO4, 2010). The study of the absorption spectra of SPEs gives decent information about the electronic states of the matrix. The optical bandgap of SPEs can be tuned by adding adequate salt' concentration to meet the precise specifications with the desired properties for a variety of optoelectronic devices that cover a broad spectrum of electromagnetic radiation (P. Sharma, V. Sharma, and S.C. Katyal, 2006) (El-Khodary, Evolution of the optical, magnetic and morphological properties of PVA films filled with CuSO4, 2010).

Figure 3-a shows the variations in absorbance (A) of pure PVA and PVA/NaI SPEs at various NaI contents as a function of wavelength. The absorbance for all films has high values at UV wavelengths in the vicinity of the fundamental absorption edge; then, the absorbance decreases with increasing wavelength to become nearly zero in the visible region because of the colourless nature of PVA. No absorbance bands in the visible region are observed due to the high transparency of the samples.

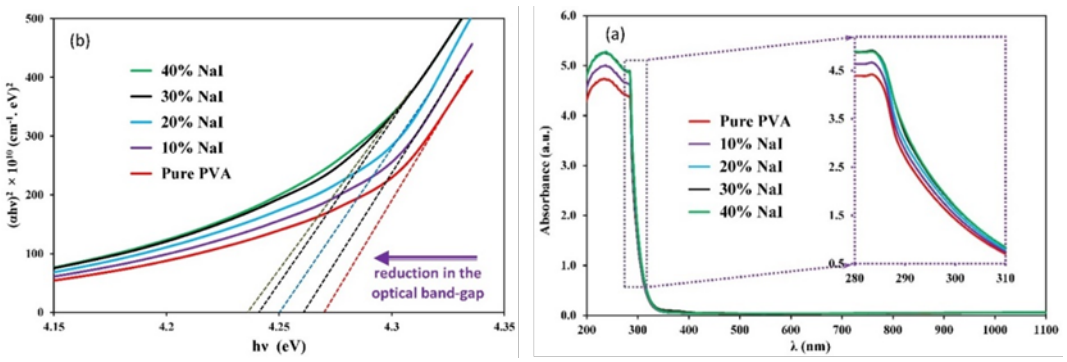

Figure 3 UV-vis absorbance spectra (a), and $(\alpha h\upsilon)^2$ versus $(h\upsilon)$ (b), for pure PVA and PVA-based sodium ion-conducting SPE with different NaI percentages.

To estimate the optical energy gap (E_g) the correlation between $(\alpha h\upsilon)^2$ versus the photon energy $(h\upsilon)$ is plotted as depicted in Fig. 3-b. According to Tauc's equation 6, the intersection of the obtained straight lines at the high absorption region, with the $h\upsilon$-axis at $(\alpha h\upsilon)^2=0$ is equal to the direct allowed E_g of the sample. It is observed that the E_g decreased with increasing NaI content in SPEs from 4.27 eV for pure PVA to 4.22 eV for SPE incorporated with 40 wt.% of NaI, as tabulated in Table 2.

Table 2 The optical parameters at 550 nm for pure PVA and SPEs incorporated with different NaI percentages.

NaI (wt.%)	α (cm^{-1})	K	n	ε_r	ε_i	E_g (eV)
0	4049	0.018	1.278	1.633	0.045	4.27
10	4331	0.019	1.289	1.661	0.049	4.26
20	4620	0.020	1.299	1.688	0.053	4.25
30	4696	0.021	1.302	1.695	0.054	4.24
40	4565	0.020	1.297	1.683	0.052	4.22

This finding can be explained in light of the fact that the band tail of localized defect states within the forbidden band gap increase with an increase in NaI content, which directly influences the decrease in the E_g of SPEs (Abdullah, 2016). Thus, the reduction in E_g forSeries of sodium-ion conducting SPEs may be understood from mobility gap variation, where the transition mainly occurs between the highest occupied molecular orbitals and the lowest unoccupied molecular orbitals rather than the transition between two extended states (valence to conduction) due to the amorphous nature of polymer (El-Khodary, Evolution of the optical, magnetic and morphological properties of PVA films filled with CuSO4, 2010).

The enhancement in the optical parameters such as absorption coefficient (α), extinction coefficient (K), refractive index (n), real (ε_r), and imaginary (ε_i) parts of optical dielectric constant, of PVA upon adding NaI at wavelength 550 nm, are depicted in Table 2. These results agree with previous reports on polymer electrolytes based on PVA (Y. Khairy, 2021).

3.3 Electrical Conductivity Analysis

Temperature-dependent DC electrical conductivity (σ_{DC}) of the PVA/NaI SPEs is investigated to probe the conduction mechanism in the investigated samples. The measured data reveals that σ_{DC} increase with an increase in NaI content due to the rise in Na^+ ions. The temperature-dependent $\sigma_{DC}$are presented as a relationship between $\ln(\sigma_{DC})$ and inverse of absolute temperature $(1000/T)$ as shown in Figure 4 The results showed that the σ_{DC} increase with increasing temperature, and verifies the Arrhenius equation. The plot's linear behavior indicates that the present system's conduction mechanism is a thermal-activated process (A.S.A. Khiar, 2010).

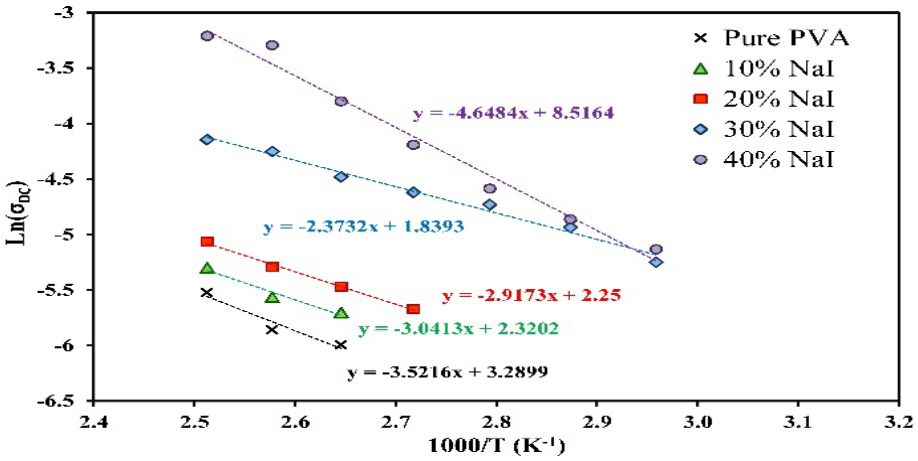

Figure 4 logarithm of DC conductivity versus reciprocal temperature for pure PVA and PVA/NaI SPEs with different NaI percentages.

The temperature-dependent σ_{DC} plot is used to extract the value of activation energy (E_A) of PVA/NaI SPEs, which can be defined as the required energy for an ion to release itself from the localized state (A.S.A. Khiar, 2010). The obtained values of E_a for pure PVA is found to be 0.304 eV and decreased with Na^+ content to reach a minimum value of 0.205 eV for PVA/NaI SPE loaded 30 wt.% NaI. Thus, the increase in σ_{DC} upon the incorporation of NaI for the current SPEs is achieved owing to an increase in both currier density and currier mobility which arises, respectively, from increases in free Na^+ and segmental mobility of PVA chains due to a decrease in the E_a.

On the other hand, the inverse relationship between σ_{dc} and E_a can be understood from the definition of conductivity which is stimulated due to a combined effect of ion density and its mobility.The inverse correlation between $\sigma_{DC}$and E_a has been monitored by many researchers for different SPEs systems (A.S.A. Khiar, 2010) (S. Diaham, M.L. Locatelli, 2012).

The variation of room-temperature AC conductivity (σ_{AC}) as a function of frequency for pure PVA and PVA/NaI SPEs is shown in Figure 5 . The σ_{AC} spectra exhibit a dispersion pattern at higher frequencies and a frequency-independent plateau region at low frequencies. The dispersed region at a high frequency usually follows Jonscher's power law, $\sigma_{AC} = A\omega^S$, where A is a constant related to the polarizability' strength, ω is the angular frequency, and S is the frequency exponent, its value varying between 0 and 1 (S. Diaham, M.L. Locatelli, 2012) (A. Arya, A.L. Sharma, 2018).

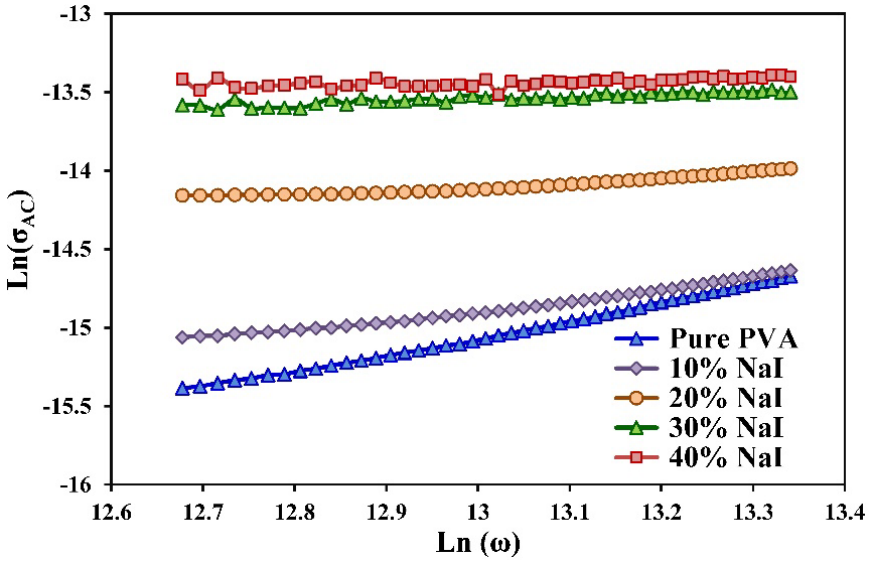

Figure 5 logarithm of AC conductivity versus reciprocal temperature for pure PVA and PVA/NaI SPEs with different NaI percentages.

It is also essential to observe that the highest NaI loading sample has the highest plateau region, and the dispersion region is shifted towards the higher frequencies. The increase in σ_{AC} with an increase in frequency for all samples, confirm that hopping conduction is the dominant mechanism (Dilip K. Pradhan, 2009) (panelAnil Kumar Bajpai, 2016).

The value of S is determined from the slope of a straight line at the high-frequency dispersion region and decreased from 0.990 for pure PVA to 0.658, 0.265, 0.155, and 0.086 for PVA/NaI SPEs incorporated 10, 20, 30, and 40 wt.% NaI, respectively. Indicating the change in the conduction mechanism from ideal Debye dielectric dipolar-type crystals ($S = 1$) for pure PVA, to ideal ionic-type crystals ($S = 0$) for SPEs at high NaI content (M. Hamzah, E. Saion, A. Kassim, M. Yousuf, 2012) (Abdulameer Khalaf Arat , Dalal Hassan Abdulkadhim , Maher Hasan Rashid, 2018) (M.S.Ahmad, A. M. Zihilif, 1992).

3.4 Gas sensor characterization

The thin film samples are deposited on a microscope slide and examined for Sensitivity, response time, and recovery time parameters that sensors are injected over the sensors at room temperature in pure PVA and with various concentrations (10 percent, 20 percent, 30 percent, and 40 percent) of NaI composite films gas sensing using NO_2.The optimum processing temperature is determined by the sensing materials and the types of gases to be studied, and it may be influenced by changes in the rates at which gas molecules adsorb and desorb on the surface of the sensor element (Mustafa, 2013).

3.4.1 At 50 ppm No_2 gas sensor

A bar graph of the film sensitivity, response time and recover time for various concentrations at various temperaturesof 323,373,423 and 573 K in NO_2 gas at a concentration of 50 ppm and the same environmental conditions is shown in Figure 6.

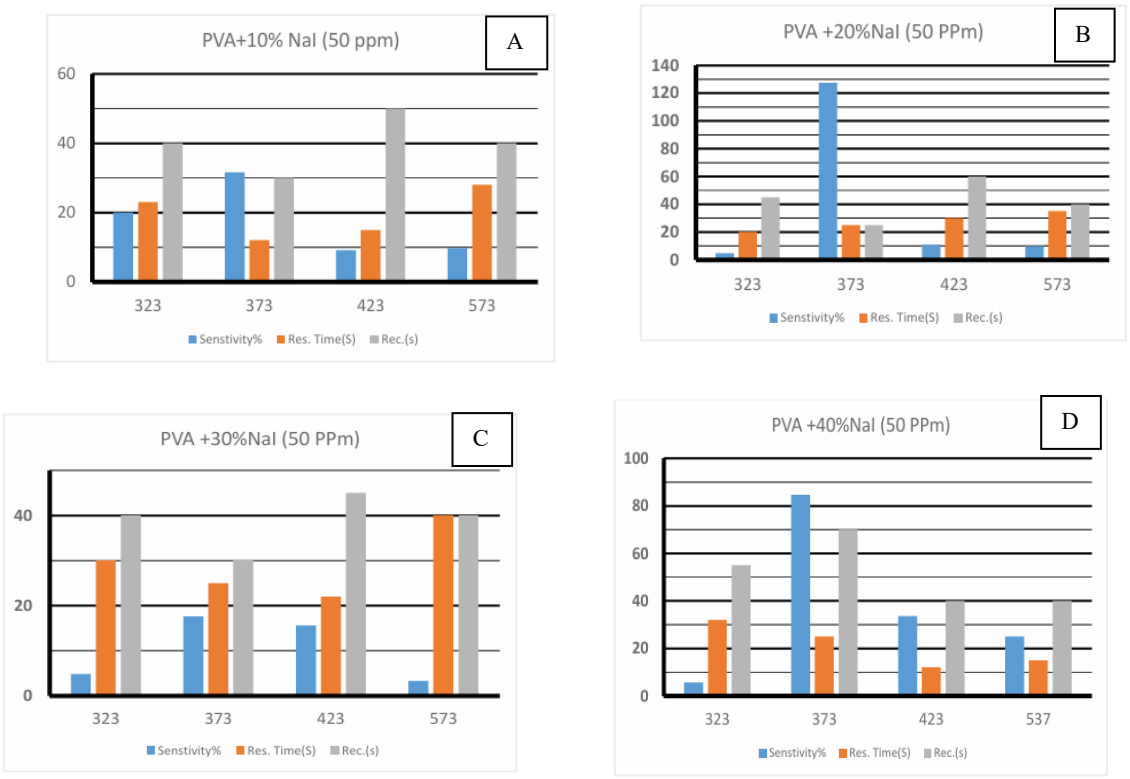

Figure 6 show the statistical value of sensitivity y, response time and recover time at (A) 10% NaI. (B) 20% NaI. (C) 30% NaI. and (D) 40% NaI at 0ppm NO2 concentration.

It is clear that the 20 wt % NaI nanocomposite exhibits the highest sensitivity to NO2 gas at a temperature of 200°C when compared to other concentrations. The reason for the reduced response time could be due to the film's surface having a smaller surface area with possible reaction sites. The NO2 gas sensor displays a strong response for NO_2 gas at a temperature of 200 oC with a rapid response and fast recovery time, and a high sensitivity of 127.3. PVA nanocomposite films with a 20 percent weight percentage of NaI are used to make it. These results indicate that this nanocomposite sensor might work well for commercial and environmental applications.

3.4.2 At 550 ppm NO_2 gas

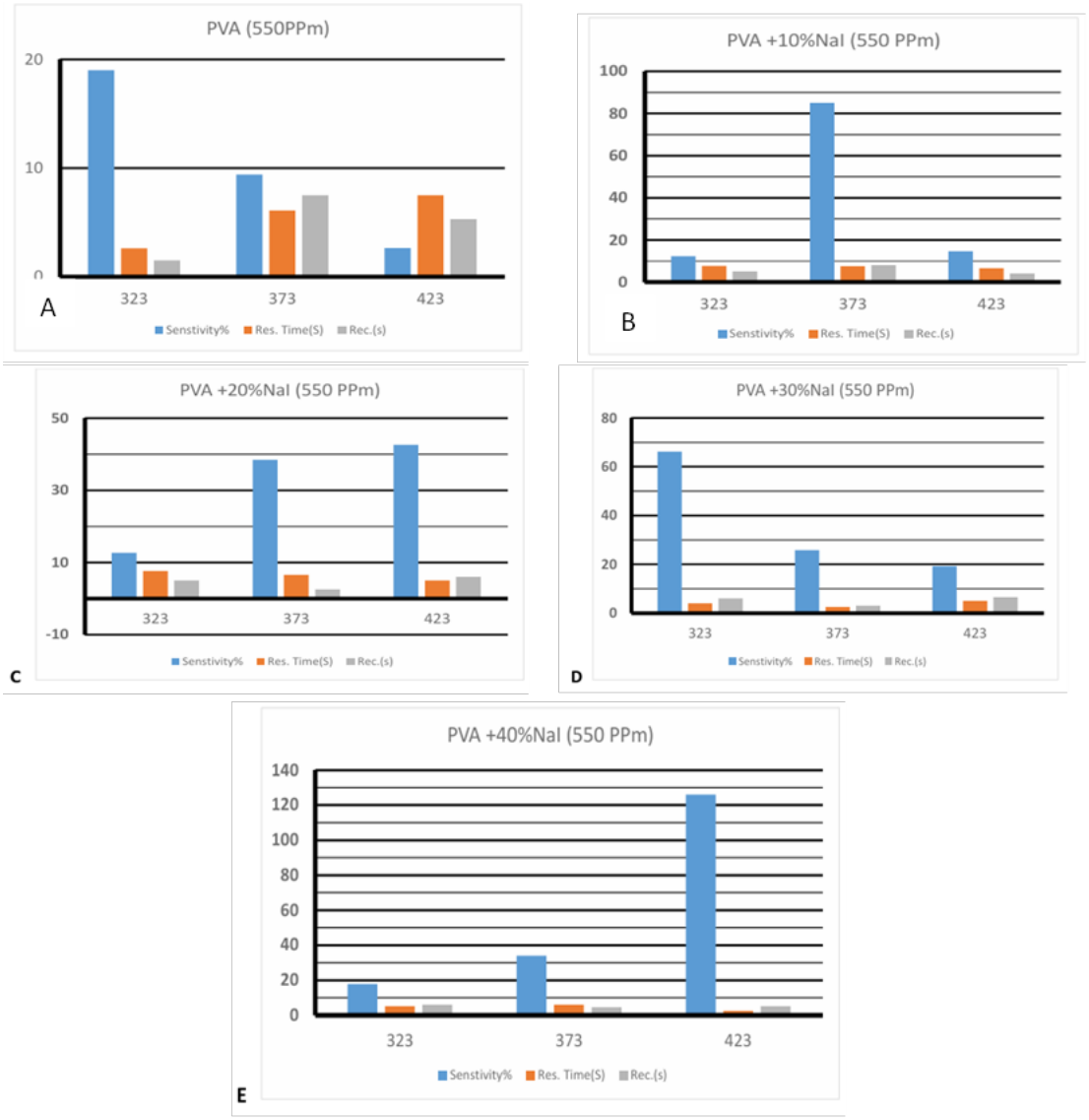

Figure 7 Statistical value of sensitivity, response time and recover time at (A) pure PVA. (B) 10% NaI. (C) 20% NaI. (D) 30% NaI. and (E) 40% NaI.

The rate of NO_2molecules interacting with the sensing surface increases at 323K, which may be mostly the result of improvements in the rate of adsorption rather than desorption. It is clear that, when compared to other concentrations, the NaI nanocomposite with a 40% percent NaI content exhibits the highest possible level of NO_2 gas sensitivity at a temperature of 423 K.

Therefore, as demonstrated by AFM experiments, the increase in particle size and surface roughness is responsible for the flms' maximal sensitivity. The sensor's response time is influenced by how fast gas molecules may diffuse and reply to the sensitive active layer. The speed of the chemical reaction on the surface grain and the speed at which gas molecules diffuse over this surface both influence sensor responsiveness. Low and high sensor temperature responses are soon constrained. Gas molecules diffuse rapidly as a result of chemical interactions and a straight surface. When the values of two processes are equivalent in a medium-speed temperature range, the sensor response is at its maximum. This mechanism suggests that the Maximum sensor response value has a specific temperature for each gas

(Ba, 2006) (Ayah F.S.Abu-Hani, FalahAwwad,Yaser E.Greish,Ahmad I.Ayesh, Saleh T.Mahmoud, 2017) (Mahdi Hasan Suhail, MohamedGhazi, Mustafa Al-hamdany, 2016).

4. CONCLUSIONS

The casting method has been used to fabricate SPE films based on PVA with varying concentrations of NaI. The XRD results revealed that the amorphous portion increases with increasing NaI concentration in the SPE films. The optical band gap of direct transition decreases from 4.27 eV for pure PVA to 4.22 eV for SPE incorporated with 40 wt.% of NaI. In contrast, the absorbance, absorption coefficient, refractive index, extinction coefficient, and optical dielectric constants increase with increasing NaI percentages in the PVA matrix. The activation energy of DC electrical conductivity decreases with the increase in NaI concentration. The frequency and NaI content increase the AC conductivity, dielectric constant, and dielectric loss of SPEs. The polar nature of PVA and salt dissociation is responsible for this behavior. The frequency-dependent AC conductivity is found to follow Jonscher's power law, and the exponent power decreases as the doping increase, indicating the change in the conduction mechanism from ideal Debye dielectric dipolar-type crystals to ideal ionic-type crystals upon loading NaI. At low gas concentrations, the PVA film showed no sensitivity to the experimental gas. The sensing method involves the gas species' ion sorption on the surface, which results in charge transfer between the surface molecules and the gas molecules and changes in electrical conductance. The oxygen's ability to remove electrons and the combustible gas' ability to restore them compete with one another. Therefore, the concentration of the combustible gas affects the metal salt's steady state value of resistance.

ACKNOWLEDGMENTS

The authors express gratitude to their respective universities for providing encouragement and infrastructure.

References

[1] A. Arya, A.L. Sharma, J. Phys.: Condens. Matter, 30 (2018) 165402
[2] A.M. Meftah, E. Gharibshahi, N. Soltani, W.M.M. Yunus, E. Saion, Polymer Composites, 6 (2014) 2435
[3] A.K. Solarajan, V. Murugadoss, S. Angaiah, J. Appl. Polym. Sci, 134 (2017) 45177
[4] A.S.A. Khiar, A.A., Ionics, 16 (2010) 123
[5] A. Khalaf Arat, D.H. Abdulkadhim, M.H. Rashid, Journal of University of Babylon, Pure and Applied Sciences, 26(6) (2018) 95
[6] O. Abdullah, J. Mater. Sci. Mater. Electron., 2 (2016) 12106
[7] A. Mohammed, M.H. Suhail, M. Ghazi, Iraqi J. Phys, 15(32) (2017) 99
[8] R. Ansar, E-J. Chem, 3 (2006) 186
[9] A.F.S. Abu-Hani, F. Awwad, Y.E. Greish, A.I. Ayesh, S.T. Mahmoud, Organic Electronics, 2 (2017) 284
[10] N. Ba, Ph.D. thesis, University of Potsdam, 2006
[11] C. Jo, D. Pugal, I.K. Oh, K.J. Kim, K. Asaka, Prog. Polym. Sci., 38 (2003) 1037
[12] D.K. Pradhan, R.C., Materials Chemistry and Physics, 115 (2009) 557
[13] A. El-Khodary, Physica B, 405 (2010) 4301
[14] A. El-Khodary, Physica B: Condensed Matter, 405(16) (2010) 4301
[15] S.R. Elliot, Adv. In Phys, 36 (1987) 135
[16] H. Yano, K. Kudo, K. Marumo, H. Okuzaki, Science Advances, 5 (2019) 1
[17] K. Balakrishnan, M. Kumar, S. Angaiah, Adv. Mater. Res., 938 (2014) 151
[18] K. Hu, D.D. Kulkarni, I. Choi, V.V. Tsukruk, Prog. Polym. Sci, 39 (2014) 1934
[19] M. Hamzah, E. Saion, A. Kassim, M. Yousuf, Malaysian Polymer Journal, 3(2) (2012) 24

[20] M. Khan, A.N. Khan, A. Saboor, I.H. Gul, Polymer Composites, 39(10) (2017) 3686
[21] M. Yu, H. Shen, Z.D. Dai, J. Bionic Eng, 4 (2007) 143
[22] M.S. Ahmad, A.M. Zihilif, Poly. Comp, 13(1) (1992) 787
[23] M.Z. Rajab, K.M. Ziadan, IOP Conference Series: Materials Science and Engineering, 928 (2020) 072038
[24] M. Mohan, V., V. Raja, A.K. Sharma, V.V.R. Narasimha Rao, Mater. Chem. Phys., 94 (2005) 177
[25] M.H. Suhail, M. Ghazi, M. Al-hamdany, International Journal of Emerging Research in Management & Technology, 5(6) (2016) 24
[26] A.A. Mohamad, Solid State Ionics, 156 (2003) 171
[27] J. Radehaus, Exp. Theo. NANOTECHNOLOGY 7 (2023) 143
[28] M. Al-hamdany, M. Ghazi, M.H. Suhail, Iraqi J. Phys, 14 (2016) 98
[29] F.A. Mustafa, Physical Sciences Research International, 1(1) (2013) 1
[30] P. Banerjee, B.M. Mandal, Synth. Met, 74 (1995) 257
[31] P. Sharma, V. Sharma, S.C. Katyal, Chalcogenide Letters, 3 (2006) 73
[32] A.K. Bajpai, R.B., Micron, 90 (2016) 12
[33] S. Diaham, M.L. Locatelli, J. Appl. Phys., 112 (2012) 013710
[34] S. Geetha, K.K. Satheesh, K. Chepuri, R.K. Rao, M. Vijayan, D.C. Trivedi, J. Appl. Polym. Sci, 112 (2009) 2073
[35] S. Virji, J. Huang, R.B. Kaner, B.H. Weiller, NanoLett, 4 (2001) 491
[36] D.J. Shirale, V.K. Gade, P.D. Gaikwad, H.J. Kharat, K.P. Kakde, P.A. Savale, S.S. Hussaini, N.R. Dhumane, M.D. Shirsat, Mater. Lett. 11 (2006) 1407
[37] L.S. Walsh, Electrical Properties of Materials, Oxford, New York, Tokyo, 1998
[38] Y. Khairy, M.M., Optik, 228 (2021) 166129
[39] X. Wang, J. Whitaker, Exp. Theo. NANOTECHNOLOGY 7 (2023) 67
[40] R. Sahnoun, Exp. Theo. NANOTECHNOLOGY 7 (2023) 78